Open access • Journal Article • DOI:10.1109/LAWP.2008.2005213

A Truncated Conical Dielectric Resonator Antenna for Body-Area Network Applications — Source link

G. Almpanis, Christophe Fumeaux, Jürg Fröhlich, Ruediger Vahldieck

Institutions: ETH Zurich, University of Adelaide

Published on: 01 Jan 2009 - IEEE Antennas and Wireless Propagation Letters (IEEE)

Topics: Dielectric resonator antenna, Monopole antenna, Coaxial antenna, Microstrip antenna and Antenna factor

A Truncated Conical Dielectric Resonator Antenna for Body-Area Network Applications

Georgios Almpanis, *Student Member, IEEE*, Christophe Fumeaux, *Member, IEEE*, Jürg Fröhlich, and Rüdiger Vahldieck, *Fellow, IEEE*

***Abstract*—An inverted truncated annular conical dielectric resonator antenna (DRA) for potential use in body-area network (BAN) applications is introduced. The antenna is designed to operate within the lower European ultrawideband (UWB) frequency band (3.4–5.0 GHz). The selected DRA geometry in combination with a capacitively loaded monopole as the feeding mechanism results in a low-profile antenna with wide bandwidth and stable monopole-like patterns. In addition, the antenna exhibits good UWB properties, as characterized through the dispersion effect on the transmitted impulse voltage signal. The DRA has been numerically and experimentally examined for both free-space and on-body applications, demonstrating a good performance in the frequency- and time-domain.**

***Index Terms*—Body-area network (BAN), dielectric resonator antennas (DRAs), ultrawideband (UWB).**

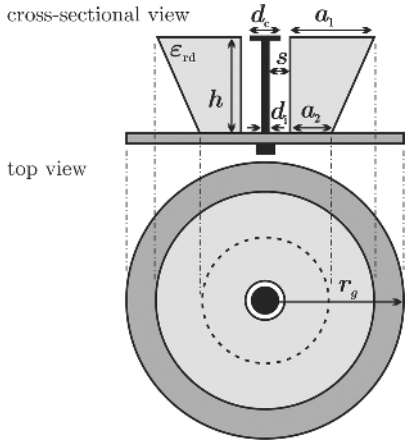

Fig. 1. Cross-sectional and top views of the inverted truncated conical DRA.

I. Introduction

DIELECTRIC resonators were first used as radiating elements two decades ago when it was demonstrated that they could exhibit low radiation Q-factors, provided they are placed in an open environment and are excited in their lower order modes [1]. Dielectric resonator antennas (DRAs) have several attractive features, such as high radiation efficiency and compact size. In addition, DRAs exhibit a wider bandwidth and a higher power-handling capability than microstrip antennas. Their versatility in shape and the variety of possible feeding mechanisms allow for better control of the excited modes and, thus, of the input impedance, the bandwidth, the polarization, and the patterns.

Based on these advantageous features, the interest in wideband linearly polarized (LP) DRAs with stable gain and radiation patterns has been growing ever since. Several approaches for bandwidth enhancement have been demonstrated [2]–[8]. They can generally be divided into two major categories. The first approach is the mode-merging technique, where multiple modes are excited and coupled at nearby frequencies [2]–[4]. In [2], a strip-fed rectangular DRA is investigated, exhibiting broadside LP radiation characteristics and a bandwidth of over 40%. The results in [2] are obtained through the excitation of the fundamental TE_{111} and the higher order TE_{113} modes of the rectangular DRA at some offset frequencies. In a similar manner, the bandwidth of probe-fed rectangular and cylindrical DRAs is increased by changing the radius-to-height and length-to-height ratios in [3]. Finally, the combination of the resonances of an annular DRA with that of a quarter-wave monopole results in a 3:1 bandwidth and monopole-like radiation patterns in [4]. In this configuration, the monopole is acting both as a loaded radiating element and a feeding structure for the dielectric resonator (DR).

The second approach for bandwidth enhancement involves reducing the radiation Q-factor of the excited DRA modes through geometrical manipulations. In [5], an aperture-coupled flipped staired-pyramid DRA is proposed, demonstrating broadside patterns and a wide impedance bandwidth. In [6], an investigation of a probe-fed trapezoidal DRA is carried out, and a comparison between the inverted trapezoids and their noninverted counterparts is made. It is finally shown that the inverted geometries are more wideband due to the smaller confinement of the electric fields inside the dielectric volume.

In this letter, the design concepts described in [4]–[6] are combined and carried a few steps further, resulting in an inverted truncated conical DRA, as sketched in Fig. 1. This antenna is promising for ultrawideband (UWB) radio applications in body-area networks (BAN) and is, therefore, subject to the following numerical investigation complemented by experimental verification.

Antenna designs for BAN applications can be quite challenging due to the lossy, dispersive propagation environment

Manuscript received June 10, 2008; revised July 25, 2008. First published September 03, 2008; current version published May 08, 2009. This work was supported by ETH Research Grant TH-38/04-1.

G. Almpanis, J. Fröhlich, and R. Vahldieck are with the Laboratory for Electromagnetic Fields and Microwave Electronics, ETH Zurich, Zurich 8092, Switzerland (e-mail: almpanis@ifh.ee.ethz.ch).

C. Fumeaux is with the School of Electrical and Electronic Engineering, The University of Adelaide, Adelaide, SA 5005, Australia (e-mail: cfumeaux@eleceng.adelaide.edu.au).

Color versions of one or more of the figures in this letter are available online at http://ieeexplore.ieee.org.

Digital Object Identifier 10.1109/LAWP.2008.2005213

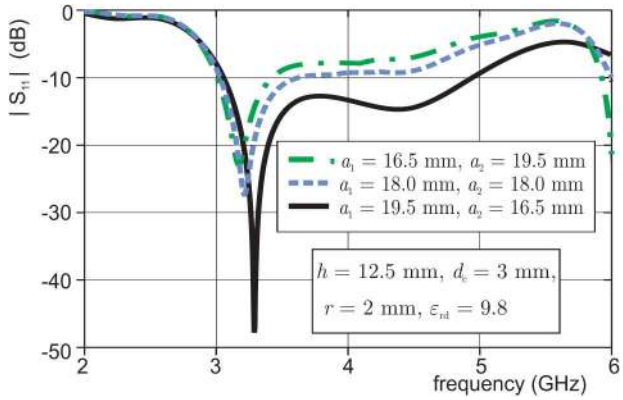

Fig. 2. Simulated return loss of the noninverted conical, cylindrical, and inverted conical DRA.

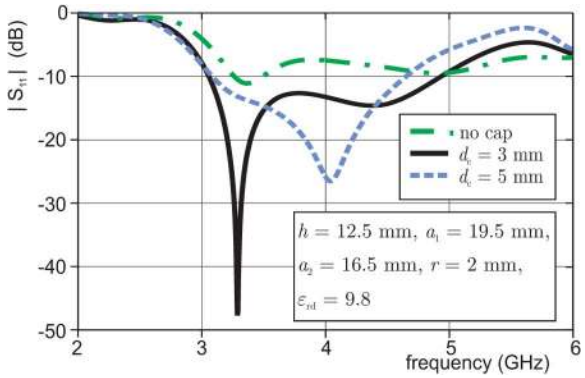

Fig. 3. Simulated return loss of the inverted truncated conical DRA for different diameters of the metallic hat.

(human skin). Moreover, requirements for large bandwidth, low signal dispersion, and stable radiation patterns are not easily met. To determine whether the proposed antenna (Fig. 1) is a good candidate to meet the specs, the DRA performance is tested both in the frequency- and time-domain. The signal dispersion effect is investigated through the measured phase of the DRA's transfer function as well as the waveform distortion between two identical DRAs used as TX and RX antennas.

II. Antenna Configuration

The DRA is intended for a specific BAN application, according to which the antenna must have a low profile and a small groundplane. Moreover, the antenna should operate in the 3.4–5.0 GHz frequency band with omnidirectional patterns. Operating as a UWB antenna requires a wide impedance bandwidth and low signal dispersion. Short pulses must be radiated with a temporal extent that is not significantly larger than that of the input signal. Furthermore, the ringing and chirp effect must be minimized [9].

The numerical analysis of the inverted truncated conical DRA was performed using two commercial full-wave analysis tools: Ansoft® HFSS employing the finite-element method (FEM) in the frequency-domain and CST® Microwave Studio using the finite-integration technique (FIT) in the time-domain. The use of two numerical tools based on different methods allows for cross-checking the accuracy of the simulations and, therefore, provides a reliable reference point before fabrication of a prototype.

The DRA configuration shown in Fig. 1 consists of an inverted truncated annular conical DR of height $h = 12.5$ mm, radii $a_1 = 19.5$ mm and $a_2 = 16.5$ mm, and dielectric permittivity $\varepsilon_{rd} = 9.8$ residing on a groundplane of radius $r_g = 30$ mm. The inverted conical shape was chosen for its wideband performance [4]–[6]. This is demonstrated in Fig. 2, where the return loss of three truncated conical DRAs of the same total volume is compared. It is evident that the inverted conical DRA ($a_1 = 19.5$ mm, $a_2 = 16.5$ mm) exhibits a wider impedance bandwidth than the cylindrical ($a_1 = a_2 = 18.0$ mm) and the noninverted conical DRA ($a_1 = 16.5$ mm, $a_2 = 19.5$ mm). It is worth mentioning here that a comparison of various types of conical DRAs was also made in [7], highlighting the advantages of the inverted conical shape. However, the DRA mode excited in [7] and the resulting radiation characteristics were different from the ones in the configuration presented here.

In the present case, the DRA was excited in the $\mathrm{TM}_{01\delta}$ mode through the center conductor of an SMA connector (diameter $d_i = 1.28$ mm) situated in the center of the DR. The distance from the outer radius of the probe to the inner surface of the DR was chosen to be different from zero ($s = 2$ mm) as a means to further enhance the DRA bandwidth [10]. The probe was capacitively loaded with a metallic hat [11] so that its height could be reduced to the height of the DR. Hence, the low DRA profile would not be distorted by the presence of the center pin. The effect of the metallic hat on the response (return loss) of the DRA is shown in Fig. 3.

A brief comparison between the DRA under investigation and the one shown in [4] demonstrates several functional and conceptual differences. One obvious difference is that there is no pin extending beyond the height of the dielectric resonator in the present DRA. Instead, a metallic cap is placed on top of the probe to maintain its electrical length after having reduced its mechanical length and to provide better matching. Therefore, a good operation can still be obtained for a DRA of a much lower profile. A further difference from [4] is that the center conductor of the SMA connector is only used to excite the DRA mode, whereas in [4] it is used both as a feeding and a resonant radiating element. The resulting 3:1 bandwidth is obtained by coupling to multiple modes at nearby frequencies. In the context of UWB operation, the excitation of multiple resonant modes creates rapid changes of the phase over frequency and look angle, thus contributing to signal dispersion. From here, it follows that the mode- merging technique is not entirely appropriate for pulsed operation. In the DRA presented here, only the $\mathrm{TM}_{01\delta}$ mode is excited, and the large bandwidth is obtained through the inverted shape of the DR. Thus, by setting the resonant frequency of the $\mathrm{TM}_{01\delta}$ mode just below the band of interest (3.4–5.0 GHz), it is possible to obtain a nearly linear phase above resonance.

III. Frequency-Domain Results

Fig. 4 shows a photograph of the antenna prototype fabricated according to the specifications given above. The return loss and the input impedance of the DRA are plotted versus frequency for free-space operation in Fig. 5, exhibiting a good agreement

Fig. 4. Realized prototype of the inverted truncated conical DRA.

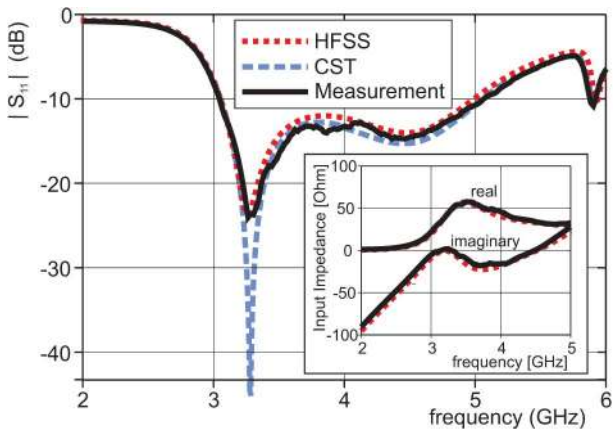

Fig. 5. Simulated and measured return loss and input impedance (inset) versus frequency of the inverted truncated conical DRA for free-space operation.

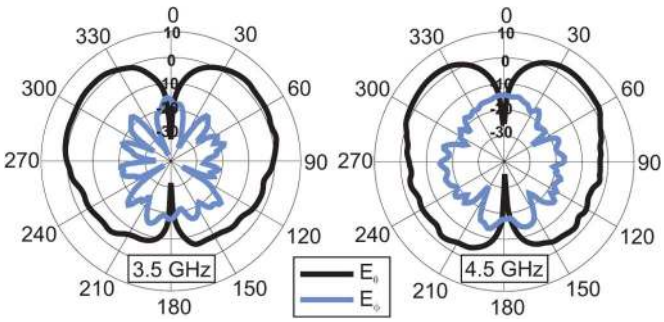

Fig. 6. Measured free-space radiation patterns for the co-(E_θ) and cross-polarization (E_φ) at 3.5 and 4.5 GHz.

between numerical and experimental results. The impedance bandwidth $(S_{11} < 10$ dB$)$ covers a frequency range between 3 and 5 GHz, with the $\mathrm{TM}_{01\delta}$ mode being resonant at 3.3 GHz. The good operation of the DRA in the aforementioned band is also evident through its measured radiation patterns (co- and cross-polarization), which are depicted in Fig. 6 at frequencies 3.5 and 4.5 GHz. It can be observed that the monopole-like patterns are reasonably stable within the entire spectrum, while the cross-polarization remains always below -15 dB.

To investigate the effect of the human body on the DRA performance, the antenna geometry was simulated using a simplified model for the human tissue (see inset of Fig. 7). The tissue was modeled as a stack of three layers: a skin layer of thickness $h_s = 1$ mm, a layer of fat with thickness $h_f = 5$ mm, and a muscle layer with $h_m = 5$ mm. The dispersive characteristics of these three layers were determined according to [12]. The model was simulated with CST, and the results were compared to measurements performed with the DRA placed on different

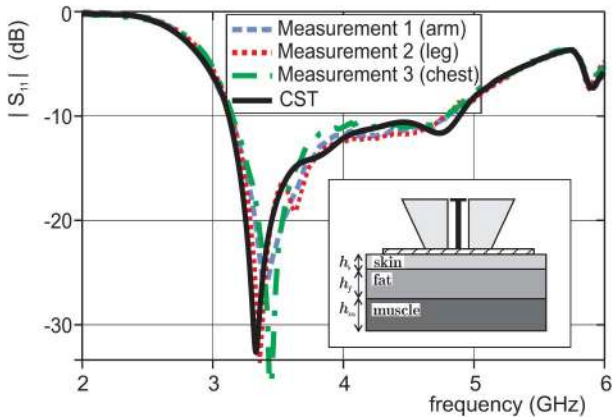

Fig. 7. Simulated and measured return loss versus frequency of the inverted truncated conical DRA for on-body operation.

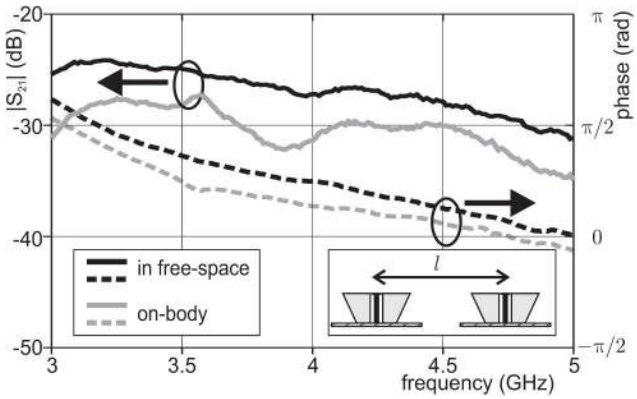

Fig. 8. Amplitude of S_{21} and phase of the transfer function of the inverted truncated conical DRA for free-space and on-body operation.

parts of the human body (arm, leg, and chest). The results are illustrated in Fig. 7, showing good agreement between simulations and measurements. From Figs. 5 and 7, it is also obvious that the effect of the tissue on the DRA performance is not that significant, at least not for the chosen size of groundplane and frequency range. The dispersive properties of the DRA were examined through measurements in the frequency- and time-domain. Considering the frequency-domain results first, the transmission coefficient S_{21} was measured in the frequency range between 3 and 5 GHz for two identical inverted truncated conical DRAs placed parallel to each other at a distance of $l = 16$ cm. A proper calibration was performed for the elimination of the dispersive effects from the connecting cables. The amplitude of S_{21} versus frequency is illustrated in Fig. 8 for both free-space and on-body transmission. It can be observed that, as expected, the path attenuation is higher in the presence of the human skin. The small instabilities in the S_{21} curve for on-body operation (compared to the more stable free-space curve) can be attributed to propagation effects on the human body.

The transfer function of the DRA can easily be extracted from the S_{21} measurements according to [13]. The phase of the transfer function for free-space and on-body operation is depicted in Fig. 8 for an electrical delay of 1 ns. It is clear that the phase characteristics exhibit a nearly linear dependency on frequency between 3.4 and 5 GHz. This linearity results in a

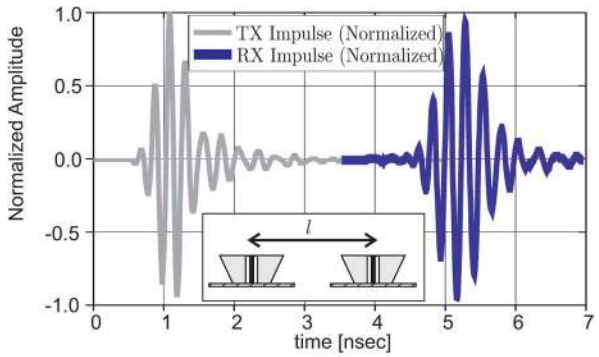

Fig. 9. Time-domain response of a pair of inverted truncated annular conical DRAs for free-space transmission.

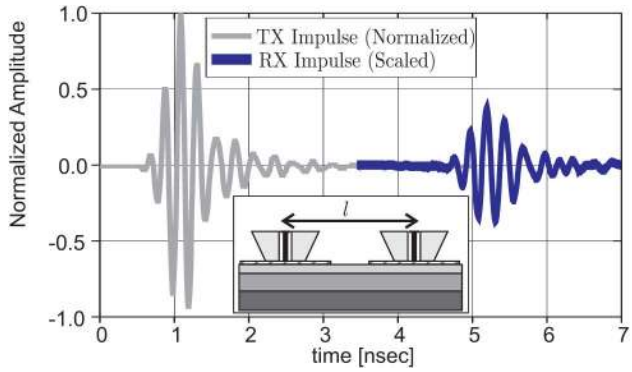

Fig. 10. Time-domain response of a pair of inverted truncated annular conical DRAs for on-body transmission.

virtually constant group delay over the spectrum, a crucial condition for good pulsed operation.

IV. Time-Domain Measurements

For the time-domain measurements, a modulated Gaussian pulse with spectral content between 3.4 and 5 GHz (defined at -3 dB level) was applied to the input of the transmitting antenna. The impulse generator consisted of a cascade of a fast triangular pulse generator and a low-pass and high-pass filter.Fig. 9 illustrates the normalized input voltage signal at the terminals of the transmitting antenna, as well as the signal received by the second antenna for transmission in free-space. The received signal is normalized to the amplitude of the transmitted signal for ease of comparison. The two identical antennas were placed parallel to each other at a distance $l = 16$ cm, as illustrated in the inset of Fig. 9. As the measurements show, the received pulse has a duration of about 1.42 ns at 10% of amplitude level, as opposed to the duration of 1.25 ns of the transmitted pulse. This temporal extension of the transmitted waveform can be considered acceptable for the intended application. Besides, other typical problems of dispersive antennas, such as ringing or chirp effects, are not distinguished here. For the case of on-body transmission, the received waveform is depicted in Fig. 10, scaled with the same normalization factor as the received signal for free-space operation. A comparison of Fig. 10 to Fig. 9 demonstrates that the received waveform for on-body transmission is very similar to the one in free-space; the sole difference is, as expected, its smaller amplitude due to the increased attenuation arising from the skin. No further deterioration of the transmitted waveform was detectable in the frequency range considered.

V. Conclusion

A low-profile inverted truncated annular conical DRA for potential use in BAN applications has been investigated both theoretically and experimentally. The basic operational concept of the DRA was described, and its performance for on-body and free-space operation was examined in the frequency- and time-domain. This antenna was intended for a particular application, but its design concepts are general. Thus, further profile reduction can be obtained by slightly increasing the dielectric permittivity of the DR or through frequency scaling.

Acknowledgment

The authors would like to acknowledge the valuable support from H.-R. Benedickter, M. Lanz, and C. Maccio.

References

[1] S. A. Long, M. W. McAllister, and L. C. Shen, "The resonant cylindrical dielectric cavity antenna," *IEEE Trans. Antennas Propag.*, vol. AP-31, no. 3, pp. 406–412, May 1983.

[2] B. Li and K. W. Leung, "Strip-fed rectangular dielectric resonator antennas with/without a parasitic patch," *IEEE Trans. Antennas Propag.*, vol. 53, no. 7, pp. 2200–2207, Jul. 2005.

[3] C. S. D. Young and S. A. Long, "Wideband cylindrical and rectangular dielectric resonator antennas," *IEEE Antennas Wireless Propag. Lett.*, vol. 5, pp. 426–429, 2006.

[4] M. Lapierre, Y. M. M. Antar, A. Ittipiboon, and A. Petosa, "Ultra wideband monopole/dielectric resonator antenna," *IEEE Microw. Wireless Compon. Lett.*, vol. 15, no. 1, pp. 7–9, Jan. 2005.

[5] R. Chair, A. A. Kishk, K. F. Lee, and C. E. Smith, "Wideband flipped staired pyramid dielectric resonator antennas," *Electron. Lett.*, vol. 40, no. 10, pp. 581–582, May 2004.

[6] G. Almpanis, C. Fumeaux, and R. Vahldieck, "The trapezoidal dielectric resonator antenna," *IEEE Trans. Antennas Propag.*, vol. 56, no. 9, pp. 2810–2816, Sep. 2008.

[7] A. A. Kishk, Y. Yin, and A. W. Glisson, "Conical dielectric resonator antennas for wide-band applications," *IEEE Trans. Antennas Propag.*, vol. 50, no. 4, pp. 469–474, Apr. 2002.

[8] S. H. Ong, A. A. Kishk, and A. W. Glisson, "Wideband disc-ring dielectric resonator antenna," *Microw. Opt. Technol. Lett.*, vol. 35, no. 6, pp. 425–428, Dec. 2002.

[9] H. Schantz, *The Art and Science of Ultrawideband Antennas*. Norwood, MA: Artech House, 2005.

[10] G. P. Junker, A. A. Kishk, A. W. Glisson, and D. Kajfez, "Effect of an air gap around the coaxial probe exciting a cylindrical dielectric resonator antenna," *Electron. Lett.*, vol. 30, no. 3, pp. 177–178, Feb. 1994.

[11] D. Lamensdorf, "Capacitatively tuned dipole," *Electron. Lett.*, vol. 9, no. 19, pp. 445–446, Sep. 1973.

[12] S. Gabriel, R. W. Lau, and C. Gabriel, "The dielectric properties of biological tissues: III. Parametric models for the dielectric spectrum of tissues," *Phys. Med. Biol.*, no. 41, pp. 2271–2293, 1996.

[13] W. Soergel and W. Wiesbeck, "Influence of the antennas on the ultra-wideband transmission," *EURASIP J. Appl. Signal Process.*, no. 3, pp. 296–305, 2005.